Sigma J Eng Nat Sci, Vol. 43, No. 3, pp. 999−1013, June, 2025

Sigma Journal of Engineering and Natural Sciences
Web page info: https://sigma.yildiz.edu.tr
DOI: 10.14744/sigma.2025.00087

Research Article

A dynamic study of the generalized Cheeger problem: An application to the temporal prediction of landslides and rainfall threshold

Praveen Kumar KUSHWAHA[1], Lakshmi Narayan MISHRA[1,*]

[1]*Department of Mathematics, School of Advanced Sciences, Vellore Institute of Technology, Vellore, Tamilnadu, 632014, India*

ARTICLE INFO

Article history
Received: 06 February 2024
Revised: 09 April 2024
Accepted: 10 June 2024

Keywords:
Dynamic Study; Generalized Cheeger Problem; Temporal Prediction of Landslides; Rainfall Threshold; Graphical Method; Landslide Predicting Parameters

ABSTRACT

This paper presents the dynamic generalized Cheeger concept, which sounds very interesting and may lead to many real-world applications in the future. This paper gives a novel insight into the dynamic generalized Cheeger problem as an application to the temporal prediction and rainfall threshold of landslides. The generalized Cheeger problem has applications in landslide modeling as it can compute the safety factor and collapse domain. Notably, the paper presents an innovative graphical method employing the dynamic generalized Cheeger concept for temporal landslide prediction and rainfall threshold determination. While developing the graphical method for temporal prediction of landslides, all causal factors of landslides are considered, and in the same graphical method, only rainfall as a causal factor of landslides is used for the threshold rainfall determination. The paper provides two numerical illustrations demonstrating the reliability and robustness of the proposed method. Moreover, the paper presents a comparative study aimed at showcasing the effectiveness of the proposed graphical method. The result of the study suggests that the rainfall threshold is lowest for circular domains among all shapes with equal area and highest for equilateral triangular domains among regular polygons of equal area, with decreasing thresholds as polygon side count increases. In conclusion, this paper introduces the dynamic study of the generalized Cheeger problem as a novel approach, proposing a graphical method for predicting temporal landslides and rainfall thresholds, ensuring promising avenues for real-life applications stemming from this dynamic study.

Cite this article as: Kushwaha PK, Mishra LN. A dynamic study of the generalized Cheeger problem: An application to the temporal prediction of landslides and rainfall threshold. Sigma J Eng Nat Sci 2025;43(3):999−1013.

INTRODUCTION

One of the most common and extensive natural disasters in the world, landslides significantly damage infrastructure, properties, and human lives [1-4]. Rainfall is the primary landslide-triggering element among all known causes, along with shallow rotational collapses and debris flows, which are also mass movement phenomena [5-7]. A translational landslide is a downslope movement of land that may happen along a particular plane surface due to

***Corresponding author.**
*E-mail address: lakshminarayan.mishra@vit.ac.in

This paper was recommended for publication in revised form by Editor-in-Chief Ahmet Selim Dalkilic

Published by Yıldız Technical University Press, İstanbul, Turkey

weakness such as a fault, joint, or bedding plane, as illustrated in Figure 1 (reproduced from [8] with permission). Due to the multidisciplinary nature of landslide prediction, a better understanding of the mechanics of landslide initiation can be achieved through the examination and analysis of each causal factor at the necessary scale and level of detail, which can also result in landslide temporal prediction and forecasting.

Landslides, snow avalanches, and other catastrophic geophysical events have been studied, modeled, and predicted in recent decades. In the physical modeling of the geologic substances involved in these unsteady events, rigid viscoplastic models are employed. These models can explain the strength (yield limit) and behavior of the material, similar to those of fluids. Models like Drucker-Prager, Bingham, etc. have a distinguishing characteristic, which is the presence of stiff (unyielded) zones close to the flow (yielded) zones. The yield limit increases, which causes the stiff zones to grow and become more capable of entirely obstructing the motion. When we do modeling of landslides, the solid or fluid is constrained by its intrinsic shape, and the initiation of the motion (onset) may be thought of as a "calamity". An investigation of stability may reveal crucial details about the "safety factor" of the natural physical structure and the beginning of motion [9-13].

A shape optimization problem could be used to describe the blocking property and the corresponding safety factor analysis [11]. The optimal shape describes the collapse domain and is connected to the beginning of the flow. The famous Cheeger problem [14], which has to do with minimizing the perimeter to area ratio of a subregion Y of region Ω, is an example of a simplified homogeneous problem. Additionally, the Cheeger problem has a wide range of applications, like in capillarity models, fracture mechanics, eigenvalue estimations [15, 16] and medical imaging. The generalized Cheeger problem is what it is termed when a problem is not homogeneous. Although the generalized Cheeger set's existence was demonstrated in [12], the uniqueness property is not universal and causes significant problems for numerical computations. In the literature, the generalized Cheeger problem has been solved numeri- cally for convex sets, but for nonconvex sets, the problem has no unique solution, making numerical computation difficult. Numerical problems with more than two solutions are called ill-posed problems. Traditional numerical methods, such as iterative algorithms or finite difference schemes, may fail to converge or produce unreliable results when applied to ill-posed problems like the generalized Cheeger problem for nonconvex sets. These methods rely on well-behaved solution spaces and smooth convergence paths, which may not exist in the presence of multiple solu- tions or poorly behaved solution spaces. Due to the non-uniqueness or instability of solutions, iterative algorithms may fail to converge on a meaningful solution. This failure occurs when the iterative process diverges or oscillates without approaching a fixed point, leading to unreliable results. In two-dimensional space, explicit constructions of the Cheeger set are known; however, they are

Figure 1. Translational landslide.

specific to convex domains, and for non-convex sets, we have little knowledge about the Cheeger set and the Cheeger constant. For more information, see [17-20]. In [21], the numerical boundary variation method was developed by using the shape derivative of the Cheeger functional to find the onset domain (generalized Cheeger set) and safety factor (generalized Cheeger constant).

We have a lot of literature on the classical Cheeger problem and its generalized counterpart in the past [12, 17-21]. The classical Cheeger problem gives static models, providing insights into optimal partitions of sets. On the other hand, the generalized Cheeger problem extends its applicability to the non-homogeneous case, serving scenes where the underlying structure displays varying mass and shear strength distributions, respectively. The current paper endeavors to bridge the gap between the static models of the generalized Cheeger problem and the dynamic nature of real-world phenomena, particularly temporal landslides (the threshold value of the single landslide triggering factor). Landslides, as complex natural phenomena influenced by various factors such as rainfall, weather conditions, rock types, and human activities, pose a significant challenge in predictive modeling [22]. While the classical Cheeger and generalized Cheeger problems traditionally operate within static frameworks, this study projects them into the dynamic domain, introducing a theoretical framework for temporal landslide prediction. Practically, landslide prediction involves a high degree of probabilistic uncertainty due to the involvement of a collection of external factors that directly influence the landslide event. However, the deterministic approach is employed here, and the current study has developed a model that can predict landslide events.

The theoretical framework model encompasses all causal factors contributing to landslides for temporal landslide prediction. Subsequently, the study filters its focus on the role of rainfall as a singular triggering factor for landslides, employing an improvised graphical method for the determination of the rainfall threshold.

The dynamic study of generalized Cheeger problems undertaken in this paper refers to the consideration of time- varying generalized Cheeger sets and constants. In the background of landslides, this implies seeking changes in generalized Cheeger sets and constants as the parameters influencing landslide prediction evolve over time due to the effects of numerous external factors. These parameters, including rainfall events, are naturally dynamic, compelling a departure from the static models commonly applied in Cheeger problem studies. The current paper asserts the importance of understanding the dynamic aspects of the generalized Cheeger problem in the domain of landslide prediction. The incentive behind this research is not only to contribute to the understanding of landslides but also to unfold the varied applications of the classical Cheeger problem in various real-life scenarios. This study develops a graphical method for rainfall threshold determination by utilizing the classical Cheeger sets and constants at specific instances of rainfall while holding other factors constant rather than generalized Cheeger sets and constants to simplify the computational complexities. This method emphasizes computational efficiency by simplifying the model. In summary, the current paper deals with an undiscovered zone by extending the static models of the generalized Cheeger problem to novel dynamic landscapes, specifically in the context of temporal landslide prediction (the threshold value of the single landslide triggering factor). The comprehensive theoretical framework for the temporal landslide prediction model developed herein not only provides insights into the intricate dynamics of landslides but also reveals the vast applicability of the Cheeger problem in numerous real-world scenarios.

The motivation behind this study stems from the pressing need to enhance our understanding and predictive ca- pabilities in landslide management. By extending the traditional static generalized Cheeger problem to a dynamic framework, this research aims to revolutionize landslide modeling and prediction methodologies. Through the devel- opment of innovative tools for temporal landslide forecasting and rainfall threshold determination, the study seeks to address critical gaps in current landslide mitigation strategies. Furthermore, the study endeavors to inspire and engage young researchers by highlighting the practical relevance of fundamental mathematical concepts, such as

J. Cheeger's geometrical optimization problem, in addressing real-world challenges. By fostering interdisciplinary exploration, this study aims to catalyze the emergence of novel applications and solutions with far-reaching impli- cations for landslide hazard management and beyond. The significance of this study lies in its pioneering approach to advancing landslide modeling and prediction through the dynamic extension of the traditional static generalized Cheeger problem. Moreover, it illuminates the intricate interplay between the geometric configurations of land formations and their susceptibility to landslides under diverse rainfall conditions. The significance of this study extends far beyond the realm of landslide modeling and prediction. By dynamically extending the traditional static generalized Cheeger problem, this research opens doors to tackling a wide array of challenges across various research domains.

The present paper is structured as follows: In the first section, preliminaries are provided as motivation, followed by a discussion of a generalized Cheeger problem. This section offers equations for the static non- planar motion of a non-homogeneous stiff visco-plastic fluid or solid, together with their corresponding variational formulations. Additionally, a shape optimization problem is used to illustrate the fluid's or solid's blocking properties. In the next section, the main content of the paper is introduced. Initially, the assumptions of the study are outlined, followed by a dynamic study of the generalized Cheeger problem. A theoretical framework for a dynamic model is then developed to predict and forecast the temporal landslide using a graphical method. The threshold value of rainfall is also calculated using this graphical method. The subsequent section provides numerical illustrations that are analyzed to assess whether a natural structure is safe over a given period of rainfall. If the structure is not safe, the rainfall threshold for a landslide is computed.

A comparative study is then presented to evaluate the effectiveness of the graphical method in landslide prediction, with a case study in the Darjeeling Himalayas, India (2010–2016). Finally, the paper presents a section on results and discussion, followed by a separate section on conclusion and future work.

PRELIMINARIES

In the preliminaries, the motivation for studying the generalized Cheeger problem and the definition of the generalized Cheeger problem are discussed. Here, a brief account of the formulation of the generalized Cheeger problem and its motivation is given; interested readers may refer to [12, 21] for details.

Motivation

Here, the equations that describe the static non-planar motion of a non-homogeneous inflexible visco-plastic fluid are analyzed in the domain

$$D = \Omega \times \mathbb{R} \subset \mathbb{R}^3, \tag{2.1}$$

where Ω is a bounded domain in $\mathbb{R}^2$ with a $W^{1,\infty}$ (Lipschitz continuous) boundary $\partial\Omega$. The simplified version for uni-directional (non-planar) motion only requires a single scalar unknown that depends on two-dimensional variables. Specifically, the static flowing velocity v is searched along the direction Oy_3 (i.e., the velocity field $\mathbf{v}$ is provided by $\mathbf{v} = (0, 0, v)$, which is independent of y_3 so that $v = v(y_1, y_2)$) (see Figure 2). The non-disappearing stress components are $\varsigma_{13}(y_1, y_2)$ and $\varsigma_{23}(y_1, y_2)$, respectively, indicated by the symbol $\boldsymbol{\varsigma} = (\varsigma_{13}, \varsigma_{23})$. (1/2) ∇v describes the rate of deformation. The constitutive equation of the fluid is as follows:

$$\begin{aligned} &\varsigma = \rho\nabla v + \frac{\gamma\nabla v}{|\nabla v|}, && if\ |\nabla v| \neq 0, \\ &|\varsigma| \leq \gamma, && if\ |\nabla v| = 0, \end{aligned} \tag{2.2}$$

where $\gamma(y_1, y_2)$ is a positive continuous function that denotes the distribution of the yield limit in D and $\rho(y_1, y_2)$ is the distribution of viscosity. The Von Mises plasticity norm for constant γ (pressure-independent plasticity) is considered here, and (2.2) recovers the traditional Bingham fluid or solid model [23, 24]. The Drucker-Prager plasticity states that for granule flows, the yield limit γ depends on pressure p linearly [11], and γ can be expressed as $\gamma = \gamma_0 + \tau p$, where $\tau = \tan a$ is the coefficient of internal friction, a is the angle of internal friction, and γ_0 is the cohesion. In the non-planar scenario, the pressure is reliant on the spatial variables since it depends on the depth and is unrelated to the velocity fields. According to this, the yield limit seems to be inhomogeneous for landslide models even for homogeneous materials [9-11]. The Eulerian coordinates for the momentum balancing law read:

$$div\varsigma + l\digamma = 0, \qquad in\ \Omega. \tag{2.3}$$

Body forces in the Y_3 direction are represented by $\digamma$, and l represents the non-dimensional loading parameter. $\digamma(y)$ can be described as $\digamma(y) = g\psi(y)\sin\theta > 0$, where g is the vertical acceleration due to gravity, $\psi(y)$ is the mass distribution function, and θ is slope angle. v_l denotes the velocity v, indicating that velocity depends on the loading parameter l.

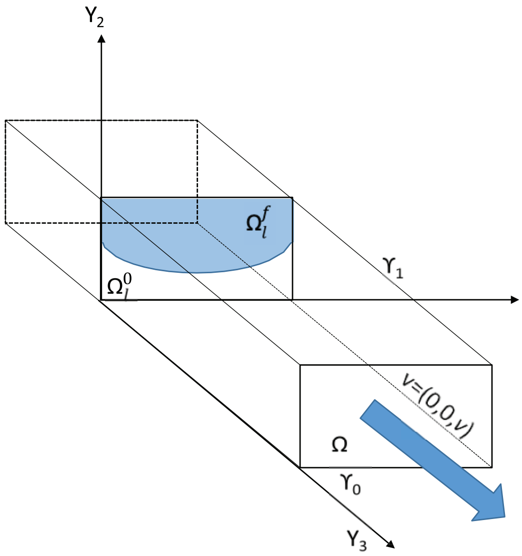

Figure 2. Non-planar geometry flow.

The boundary of Ω is divided into two parts as $\Upsilon = \Upsilon_0 \cup \Upsilon_1$ so that the equations (2.2) and (2.3) can be completed with some boundary conditions. An adherence condition on Υ_0 is considered here, and Υ_1 is considered a stress-free surface (rigid roof). Stating clearly,

$v_l = 0$ on Υ_0, $\boldsymbol{\varsigma}.\mathbf{n} = 0$ on Υ_1,

where $\mathbf{n}$ represents outward unit normal on $\partial\Omega$.

It is assumed in the following that

$$\gamma \in C^1\left(\bar{\Omega}\right), \digamma, \rho \in C^0\left(\bar{\Omega}\right), \gamma(Y) \geq \gamma_1 > 0,$$
$$\rho(Y) \geq \rho_0 > 0, \forall Y \in \Omega$$

Defining,

$E = \{e \in H^1(\Omega) | e = 0 \text{ on } \Upsilon_0\}.$

Hence, the non-planar flow variational formulation is

$$v_l \in E, \quad \int_\Omega \rho(Y)\nabla v_l(Y).\nabla(e(Y) - v_l(Y))dY \\ + \int_\Omega \gamma(Y)|\nabla e(Y)|dY - \int_\Omega \gamma(Y)|\nabla v_l(Y)|dY \\ \geq l\int_\Omega \digamma(Y)(e(Y) - v_l(Y))dY, \forall e \in E. \tag{2.4}$$

The mentioned problem is a classic variational inequality that may be expressed as an energy minimum problem.

$$\tau(e) = \frac{1}{2}\int_\Omega \rho|\nabla e|^2 + \int_\Omega \gamma|\nabla e| - l\int_\Omega \digamma e, e \in E.$$

A unique solution v_l will be obtained if $meas(\Upsilon_0) > 0$. The sufficient conditions for the existence of a solution are $\Upsilon_0 = \emptyset$ and $\int_\Omega \digamma(Y)dY = 0$, and up to an additive constant, the solution is unique. The former will always be assumed to be true in the following; the other can be derived with obvious, slight modifications.

Assuming, $\Omega_l^0 = \{Y \in \Omega | v_l(Y) = 0\}$, $\Omega_l^f = \{Y \in \Omega | v_l(Y) \neq 0\} = \Omega - \Omega_l^0$.

Ω_l^0 and Ω_l^f are the families of subdomains of Ω where fluid is stationary and moving, respectively. In landslip modeling, the blocking phenomena assure the stability of the rest configuration and can be represented as follows:

The fluid is obstructed if $v_l \equiv 0$ is a solution of (2.4) (see [11, 12]). Therefore, it gives $\Omega_l^0 = \Omega$, $\Omega_l^f = \emptyset$.

The following optimization problem can represent the blocking property for the function $T : E \to \mathbb{R}$ as follows:

$$\lambda = \inf_{e\in E} T(e), \qquad T(e) = \frac{\int_\Omega \gamma(Y)|\nabla e(Y)|dY}{|\int_\Omega \digamma(Y)e(Y)dY|}, \tag{2.5}$$

where λ denotes the safety factor of the natural structure during a landslide. The necessary and sufficient condition for blocking fluid ($v_l \equiv 0$, i.e., $\Omega_l^0 = \Omega$) is $l\lambda \geq 1$.

Generalized Cheeger Problem

Let $\Lambda: S^* \dashrightarrow R$ be the function defined from set S^* to set of real numbers, where S^* is the set of all open subsets (w) of Ω with a finite perimeter and regular boundary, and

$$\Lambda(w) = \frac{\int_{\partial\omega\setminus\Upsilon_1} \gamma(Y)dS}{|\int_\omega \digamma(Y)dY|}. \tag{2.6}$$

The shape optimization problem:

$$\lambda = \Lambda(w*) = \min_{w\in S*} \Lambda(w) \tag{2.7}$$

is called the generalized Cheeger problem. The optimal set w^* (generalized Cheeger set of Ω) denotes the part of the domain Ω from where landslides will occur if parameter l exceeds λ (generalized Cheeger constant of Ω).

More accurately,

$$w* = \lim_{l\to S^+} \Omega_l^f = \Omega - \lim_{l\to S^+} \Omega_l^0, \tag{2.8}$$

where w^* is a solution to the shape optimization problem (2.7).

Observing that for $\digamma \equiv \gamma \equiv 1$ and $\Upsilon_1 = \emptyset$. Then, the generalized Cheeger problem reduces to the classical Cheeger problem:

$$\lambda_c = \Lambda_c\left(w \underset{c}{*}\right) = \min_{w\in S*} \Lambda_c(w), \tag{2.9}$$

$$\Lambda_c(w) = \frac{\int_{\partial\omega} dS}{\int_\omega dX}, \tag{2.10}$$

where $w*_c$ denotes the Cheeger set and λ_c denotes the Cheeger constant of the domain Ω, respectively.

THEORETICAL FRAMEWORK MODEL OF TEMPORAL LANDSLIDE PREDICTION AND CALCULATION OF RAINFALL THRESHOLD VIA GRAPHICAL METHOD BY USING A DYNAMIC STUDY OF THE GENERALIZED CHEEGER CONCEPT

Assumptions Underlying the Study

Here are the assumptions of the study listed pointwise:

1. At each instant of time, the value of the landslide-predicting parameters of the current study can be calculated, which depend on m number of external factors of the landslide.
2. The graphical method for the determination of the threshold value of the triggering factor is effective when there exists a known relationship between the landslide-predicting parameters integral to the present study and the specific triggering factor in question.
3. In rainfall threshold determination, only rainfall is considered the landslide-triggering factor.
4. While computing the rainfall threshold, only the rainfall amount per event is considered, and all other characteristics of the rainfall event are taken as constants.
5. The parameter l and bulk density of the soil are assumed to be the only parameters that are changing due to the rainfall event, and all other parameters of the present study are taken as constants in the development of the graphical method for rainfall threshold.
6. The mass distribution over a cross-sectional area of domain D is assumed to be constant and increases linearly with depth l due to gravity.
7. The mass density of a piece of land (domain D) increases linearly with the rainfall amount P.
8. The parameter gravity g considered constant throughout the whole study.

Dynamic Generalized Cheeger Concept

In this section, we introduce the dynamic generalized Cheeger concept, focusing on a three-dimensional plate denoted as $\mathbb{P}$. Defined as the Cartesian product of a bounded domain Ω in $\mathbb{R}^2$ with a Lipschitz continuous boundary $\partial\Omega$ and the entire real line $\mathbb{R}$:

$$\mathbb{P} = \Omega \times \mathbb{R} \subset \mathbb{R}^3. \tag{3.1}$$

Here, Ω represents a confined region with a $W^{1,\infty}$ (Lipschitz continuous) boundary, ensuring structural integrity. The functions $f(x, y, z)$ and $g(x, y, z)$ characterize the shear strength distribution and mass distribution across the three-dimensional plate $\mathbb{P}$, respectively. The shape of the plate is denoted as $S(\mathbb{P})$. Our exploration centers around the dynamic generalized Cheeger problem, investigating the behavior of the generalized Cheeger set and constant concerning temporal variations in the plate's shape, shear strength distribution function $f(x, y, z)$, and mass distribution function $g(x, y, z)$, and inferring some important and interesting information about the system under study.

The dynamic generalized Cheeger concept opens routes for studying the impact of evolving parameters on the plate's Cheeger characteristics. This dynamic inquiry may extend beyond regular applications, illustrating its adaptability beyond landslide phenomena. The dynamic study of the generalized Cheeger problem is poised to yield worthwhile insights transcending disciplinary bounds. The potential real-life applications of the dynamic generalized Cheeger concept may be vast and diverse. In this paper, we delve into one specific application: the temporal prediction of landslides and rainfall thresholds. This analysis represents a practical manifestation of the vast applicability of the dynamic generalized Cheeger concept, demonstrating its importance in responding to real-world challenges and forecasting geological events with implications beyond the immediate scope of traditional Cheeger problems.

The choice of natural calamities like rainfall and landslides for Cheeger's study stems from their direct relevance to geometric analysis and their significant impact on human lives and infrastructure. By focusing on these phenomena, researchers can employ geometric concepts such as the Cheeger constant to assess landslide susceptibility, predict critical rainfall thresholds, and form disaster management strategies. Narrow examples include using the Cheeger problem to analyze specific landslide-prone regions, optimizing road infrastructure designs to mitigate landslide risks, developing early warning systems based on rainfall thresholds, implementing land use regulations in vulnerable areas, and designing slope stabilization measures to enhance resilience to natural hazards. These applications showcase the practical utility of the Cheeger problem in addressing specific challenges associated with rainfall-induced landslides, contributing to more effective risk assessment, mitigation, and disaster response efforts.

Theoretical Framework Model for Temporal Landslide Prediction Using a Graphical Method

Landslide phenomena are intricately linked to numerous external factors, such as rainfall, weather conditions, and human activities (refer to A.1 in Appendix A for details). These factors evolve over time, creating conducive conditions for landslides. Consider a hypothetical natural structure with the cuboidal domain under investigation (see Figure 5).

From the preliminary section, the landslide-predicting parameters of the present study are defined as follows:

1. $\gamma(x)$: Function describing the yield limit distribution over the domain D.
2. $\psi(x)$: Function describing the mass distribution over the domain D.
3. X: Angle of slope.
4. l: Loading parameter.
5. $S(D)$: Shape of the domain D.
6. g: Vertical acceleration due to gravity.

As external factors influencing landslide phenomena change, the landslide-predicting parameters of the present study also change. A brief account of the dependence of parameters on external factors causing landslides is given in A.2 in Appendix A.

Let the temporal landslide prediction be conducted in the domain D within the hypothetical natural structure. Consider the time interval $[0, T]$, and let $P[0, T] = \{t_1, t_2, t_3,..., t_n\}$ represent a partition of this interval into n instants of time, where $0 = t_1 < t_2 < t_3 <...< t_n = T$.

Let $F = \{f_1, f_2, f_3,..., f_m\}$ be a collection of all external factors contributing to a landslide. It is assumed that at each instant of time t_i (where $i \in \{1, 2, 3,..., n\}$), the value of landslide predicting parameters can be calculated, which depend on m number of external factors of the landslide.

Let the following values of landslide predicting-parameters at each instant t_i:

1. $l_t i\,(f_1, f_2, f_3,..., f_m)$, where, $t_i \in P[0, T]$ and $f_j \in F$, $\forall\, j \in \{1, 2, 3,..., m\}$.
2. $X_t i\,(f_1, f_2, f_3,..., f_m)$, where, $t_i \in P[0, T]$ and $f_j \in F$, $\forall\, j \in \{1, 2, 3, ..., m\}$.
3. $\gamma_t i\,(x)(f_1, f_2, f_3,..., f_m)$, where, $t_i \in P[0, T]$ and $f_j \in F$, $\forall\, j \in \{1, 2, 3,..., m\}$.
4. $\psi_t i\,(x)(f_1, f_2, f_3,..., f_m)$, where, $t_i \in P[0, T]$ and $f_j \in F$, $\forall\, j \in \{1, 2, 3,..., m\}$.
5. $S_t i\,(D)(f_1, f_2, f_3,..., f_m)$, where, $t_i \in P[0, T]$ and $f_j \in F$, $\forall\, j \in \{1, 2, 3,..., m\}$.
6. g (considered to be constant).

The study of landslide phenomena with varying g is beyond the scope of the present study.

The generalized Cheeger constant λ and generalized Cheeger set $C(D)$ of the given domain D can be calculated by using the numerical boundary variation method given in [21].

Let λ_i be the value of the generalized Cheeger constant of $S_t i\,(D)$ at instant t_i $\forall\, i \in \{1, 2, 3, ..., n\}$.

Let l_i be the value of parameter l at instant t_i $\forall\, i \in \{1, 2, 3, ..., n\}$.

Now, two sets S_1 and S_2 of n two tuple points (t_i, λ_i) and (t_i, l_i) in R^2 are generated, respectively, as given below:

$S_1 = \{(t_i, \lambda_i) : i \in \{1, 2, 3,..., n\}\}$ and $S_2 = \{(t_i, l_i) : i \in \{1, 2, 3,..., n\}\}$.

Plotting the points of sets S_1 and S_2 in R^2 and fitting the curves by using appropriate software.

Result

A landslide is anticipated to occur approximately at time instant t_f when the curve associated with parameter l surpasses the curve associated with λ for the first time, and the onset flow region is the generalized Cheeger set $C_t f(D)$ of the $S_t f(D)$, where $S_t f(D)$ is the shape of domain D at time instant t_f.

Below, the results are shown graphically with hypothetical numerical values for sets S_1 and S_2, respectively. Here, Figure 3 shows the graph corresponding to Table 1, and hence the natural structure is safe as the curve associated with parameter l is not above the curve associated with λ.

Table 1. Hypothetical numerical values of set S_1 and set S_2

t_i:	200	400	600	800	1000
λ_i:	$2.1 * 10^8$	$2.25 * 10^8$	$3.9 * 10^8$	$6.2 * 10^8$	$12.1 * 10^8$
l_i:	$1.1 * 10^8$	$1.25 * 10^8$	$1.6 * 10^8$	$1.95 * 10^8$	$2.1 * 10^8$

Table 2. Hypothetical numerical values of set S_1 and set S_2

t_i :	200	400	600	800	1000
λ_i :	$0.25 * 10^9$	$0.3 * 10^9$	$0.4 * 10^9$	$0.6 * 10^9$	$1.2 * 10^9$
l_i :	$0.12 * 10^9$	$0.3 * 10^9$	$0.45 * 10^9$	$0.8 * 10^9$	$1.7 * 10^9$

Here, Figure 4 shows the graph corresponding to Table 2, and hence a landslide is anticipated to occur approximately at $t = 500$ units (intersection point of curve l and curve λ), where the curve associated with parameter l surpasses the curve associated with λ for the first time.

In our graphical method, we illustrate the relationship between λ and l over time, acknowledging that each time instant (t) encapsulates the values of these predictive parameters, contingent upon the fluctuating external factors. These external factors evolve over time, creating conducive conditions for landslides. Thus, by plotting these graphs across time, our theoretical model for temporal landslide prediction encompasses the entirety of causal factors, ensuring a comprehensive and robust approach to landslide forecasting.

Rainfall Threshold Using a Graphical Method

In the context of a singular landslide triggering factor, the determination of the threshold value for the occurrence of a landslide becomes feasible through the utilization of a proposed graphical method. This method proves effective when there exists a known relationship between the landslide-predicting parameters integral to the present study and the specific triggering factor in question. The focus of this approach is on the rainfall threshold, with considerations limited solely to rainfall as the triggering factor.

The rainfall threshold is characterized as the minimum amount of rainfall necessary to initiate landslide phenomena. This research employs a graphical method tailored to assess and quantify this threshold, emphasizing the pivotal role of rainfall in triggering landslides. The effectiveness of this graphical method is contingent upon accurate data concerning landslide-predicting parameters and their correlation with rainfall.

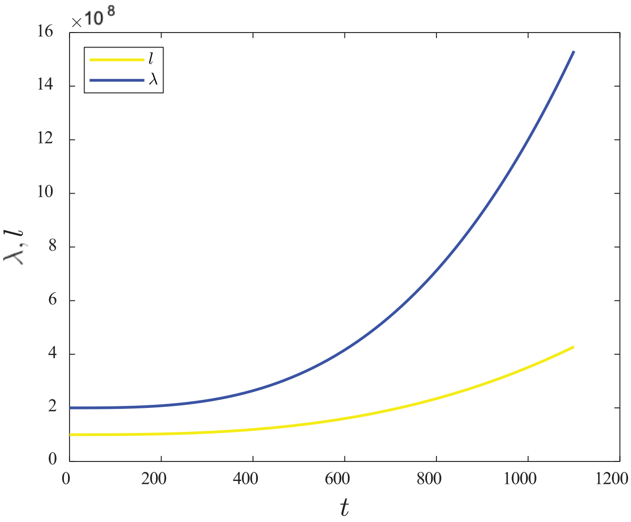

Figure 3. Graph of λ, l with respect to t.

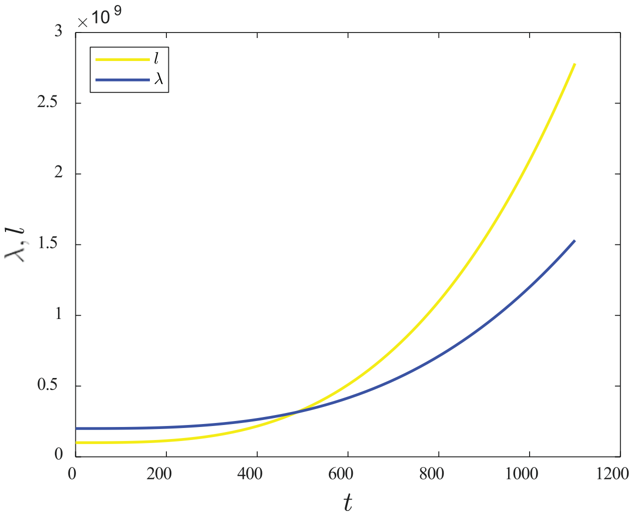

Figure 4. Graph of λ, l with respect to t.

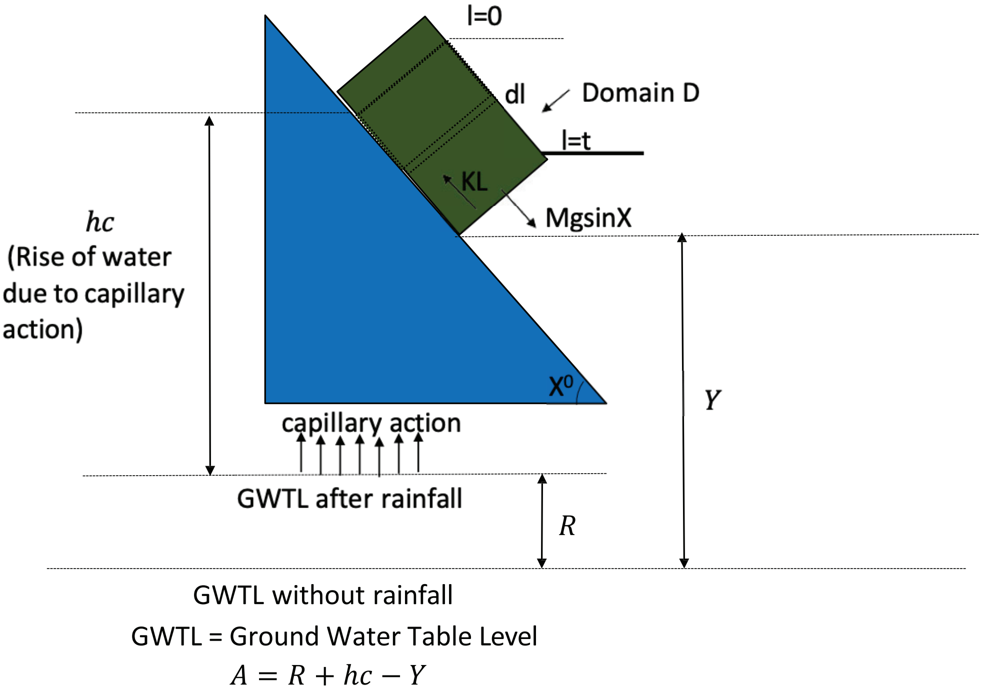

Figure 5. Mechanism of landslide due to rainfall shown in the hypothetical natural structure.

In the analysis of rainfall thresholds for domain *D* within a hypothetical natural structure (see Figure 5), the domain is envisioned as being partially filled with geologic material demonstrating semi-fluid characteristics. The parameter l signifies the level ($l = 0$ to $l = t$) of the geologic material within domain *D* (see Figure 5).

Mechanics of Domain *D*

The force (weight) $Mg \sin X$ is exerted by the geologic material (semi-fluid) on the bottom surface (rectangular plane) of domain *D* in the downward direction parallel to the inclined plane (see Figure 5), where,

M: Mass of the geologic material (semi-fluid).

X: Angle of slope.

g: Vertical acceleration due to gravity.

The shear force *KL* is the counter force for the weight $Mg \sin X$ exerted on the bottom surface of the domain *D* in the upward direction parallel to the inclined plane (see Figure 5). Where,

K: Yield limit per unit length present on the bottom surface of domain *D*. *L*: The perimeter of the collapse subdomain of domain *D*.

For unstable natural structures, the inequality of forces is given as:

$$Mg \sin X > KL. \tag{3.2}$$

While computing the rainfall threshold, only the rainfall amount per event is considered, and all other characteristics of the rainfall event are taken as constants. The rainfall event increases the groundwater table, and due to capillary action, the water rises to the cuboidal domain *D*, which increases the value of parameter l and increases the mass of the geologic material, leading to landslides as shown in Figure 6, where a brief account of the relationship of landslide-predicting parameters with rainfall is given [25-29]. The relationship (regression model) between rainfall (*P* in *mm*) and groundwater table (*R* in *m*) is taken as $R = 0.0018P - 0.0193$ with rainfall amount ranges from 39 to 1410 in *mm* and a strong linear relationship (correlation = 0.96) of the site named Jiuqu of the Dashu district, of Kaohsiung city, Southern Taiwan [27].

It is assumed here that parameters l and bulk density of the soil are the only parameters that are changing due to the rainfall event, and all other parameters of the present study are taken as constants in the development of the graphical method for rainfall threshold.

The calculation of mass (*M*) of the geologic material contained in domain *D* from region $l = 0$ to $l = t$ appeared in inequality 3.2:

The mass distribution over a cross-sectional area of domain *D* is assumed to be constant and increases linearly with depth l due to gravity. It is also assumed that the mass density of a piece of land (domain *D*) increases linearly with the rainfall amount *P*. Thus, mass density at the cross-sectional area at the depth l at rainfall *P* is $a + bP + cl$, where $(a, b, c) \in R^3_+$. Let dM be the mass of a small portion dD (with volume $dl * A$) at rainfall *P* and at depth l of domain *D*, where dl is an infinitesimally small length and *A* is the cross-sectional area of domain *D* (see Figure 5).

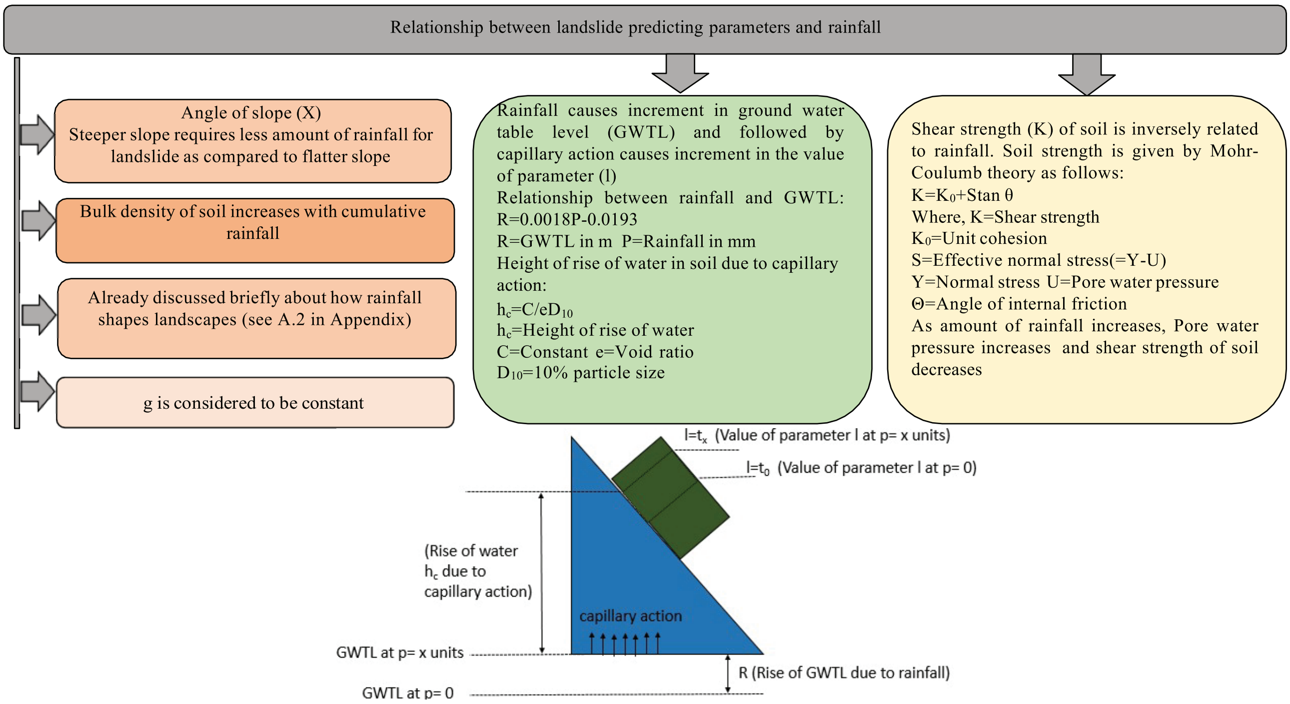

Figure 6. Relationship of landslide-predicting parameters with rainfall.

Therefore,

$$
\begin{aligned}
M &= \int_0^t (a + bP + cl)\, Adl \\
&= \int_0^t a\, Adl + \int_0^t b\, PAdl + \int_0^t c\, lAdl \\
&= [aAl]_0^t + [bPAl]_0^t + [cAl^2/2]_0^t \\
&= aA(t-0) + bPA(t-0) + \frac{cA(t^2-0)}{2} \\
&= aAt + bPAt + \frac{cAt^2}{2}.
\end{aligned}
$$

Now, from inequality (3.2),

$$\left(aAt + bPAt + \frac{cAt^2}{2}\right) g\sin X > KL$$

$$\left(aAt + bPAt + \frac{cAt^2}{2}\right) g\sin X - KL > 0$$

$$\frac{cAg\sin X}{2} t^2 + [bPAg\sin X + aAg\sin X]t - KL > 0$$

$$t > \frac{-\left[bPAg\sin X + aAg\sin X + \sqrt{(bPAg\sin X + aAg\sin X)^2 + 2AcgKL\sin X}\right]}{cAg\sin X},$$

and

$$t > \frac{-(bPAg\sin X + aAg\sin X) + \sqrt{(bPAg\sin X + aAg\sin X)^2 + 2AcgKL\sin X}}{cAg\sin X},$$

or

$$t < \frac{-\left[bPAg\sin X + aAg\sin X + \sqrt{(bPAg\sin X + aAg\sin X)^2 + 2AcgKL\sin X}\right]}{cAg\sin X},$$

and

$$t < \frac{-(bPAg\sin X + aAg\sin X) + \sqrt{(bPAg\sin X + aAg\sin X)^2 + 2AcgKL\sin X}}{cAg\sin X}.$$

The acceptable value of t is as follows:

$$t > \frac{-(bPAg\sin X + aAg\sin X) + \sqrt{(bPAg\sin X + aAg\sin X)^2 + 2AcgKL\sin X}}{cAg\sin X},$$

$$t > (a - bP)/c + \sqrt{(bP + a)^2/c^2 + \frac{2KL}{cAg\sin X}}.$$

Let $\lambda = \min\{(a - bP)/c + \sqrt{(bP + a)^2/c^2 + \frac{2KL}{cAg\sin X}}\}$.

Thus, $\lambda = \{(a - bP)/c + \sqrt{(bP + a)^2/c^2 + \frac{2K}{cg\sin X}\min\left(\frac{L}{A}\right)}\}$.

Hence,

$$\lambda = \{(a - bP)/c + \sqrt{(bP + a)^2/c^2 + \frac{2K}{cg\sin X} h(\Omega)}\}, \quad (3.3)$$

where $h(\Omega)$ is Cheeger constant of the rectangular plane Ω (bottom surface of domain D). Using the formula for the Cheeger constant of the rectangle as follows:

$$h(\Omega) = \frac{4 - \pi}{(\alpha + \beta) - \sqrt{(\alpha - \beta)^2 + \pi\alpha\beta}}, \quad (3.4)$$

where α and β are the breadth and length of the rectangular plane Ω, respectively. A Landslide will occur when $t > \lambda$. Thus, λ will be treated as a safety factor for the domain D. Let $\mathcal{R} = [I_1, I_2]$ be the range of rainfall amount and $\mathcal{P} = \{P_1, P_2, P_3,..., P_n\}$ denotes the n data set of rainfall amount after doing a partition of the range of amount of rainfall. Let l_i be the value of parameter l at rainfall P_i, and from Figures 5 and 6, the equation for l_i is given as follows:

$$A = R + h_c - Y,$$

$$\sin X = \frac{A}{l} \Rightarrow l = \frac{A}{\sin X},$$

$$\text{Thus } l_i = \frac{R_i + h_c - Y}{\sin X} = \frac{0.0018P_i - 0.0193 + \frac{C}{eD_{10}} - Y}{\sin X}.$$

Let λ_i be the value of λ at rainfall P_i, and it can be calculated from the equations (3.3) and (3.4). Now, two sets S_3 and S_4 of n two tuple points (P_i, λ_i) and (P_i, l_i) in R^2 are generated, respectively, as given below:

$S_3 = \{(P_i, \lambda_i) : i \in \{1, 2, 3,..., n\}\}$ and $S_4 = \{(P_i, l_i) : i \in \{1, 2, 3,..., n\}\}$.

Plotting the points of sets S_3 and S_4 in R^2 and fitting the curves by using appropriate software.

Result

The rainfall threshold is approximately P_f, the amount of rainfall when the curve associated with the parameter l surpasses the curve associated with safety factor λ for the first time.

$$\lambda = \{(a - bP)/c + \sqrt{(bP + a)^2/c^2 + \frac{2K}{cg\sin X} h(\Omega)}\}. \quad (4.1)$$

$$h(\Omega) = \frac{4 - \pi}{(\alpha + \beta) - \sqrt{(\alpha - \beta)^2 + \pi\alpha\beta}}. \quad (4.2)$$

$$l = \frac{R + h_c - Y}{\sin X}. \quad (4.3)$$

Where,

$$R = 0.0018P - 0.0193. \quad (4.4)$$

$$h_c = \frac{C}{eD_{10}}. \quad (4.5)$$

Let the values of variables that appeared in equations (4.1)–(4.5) be: $(a, b, c) = (5, 8, 1)$, $K = 15\ N/m$, $g = 9.8\ m^2/s$, $X = 30$, $\alpha = 1$, $\beta = 2$, $C = 5 \times 10^{-5}\ m^2$, $e = 0.35$, $D_{10} = 4 \times 10^{-4}\ mm$, $Y = 0.6\ m$.

The following table is obtained by substituting the above values of variables in the expressions of λ and l with each value of rainfall amount taken from the set P:

Fitting the curve after plotting the points in Table 3 by using Matlab software. As the curve associated with parameter l is not above the curve associated with safety factor λ, the natural structure is safe over the whole time duration of rainfall (see Figure 7).

Table 3. Hypothetical numerical values of set S_3 and set S_4

P_i :	$P_1 = 200$	$P_2 = 400$	$P_3 = 600$	$P_4 = 800$	$P_5 = 1000$
λ_i :	$\lambda_1 = 10.0052$	$\lambda_2 = 10.0021$	$\lambda_3 = 10.0014$	$\lambda_4 = 10.0013$	$\lambda_5 = 10.0010$
l_i :	$l_1 = 0.6977$	$l_2 = 1.0577$	$l_3 = 1.4177$	$l_4 = 1.7777$	$l_5 = 2.1377$

NUMERICAL ILLUSTRATIONS

In this section, two numerical illustrations are given. In the first numerical illustration, the natural structure is safe over the whole period of rainfall, and in the second numerical illustration, the rainfall threshold is calculated. The graphical method for calculating the rainfall threshold has been developed in Subsection 3.3 and also given how rainfall causes the landslide.

Illustration 1

The range of the rainfall amount is taken as R = [39 mm, 1100 mm], and the partition of the range of the rainfall amount is given as P = {200, 400, 600, 800, 1000}.

The expressions for safety factor λ and parameter l, respectively, can be written from equations (3.3) and (3.4) and Figures 5 and 6 as follows:

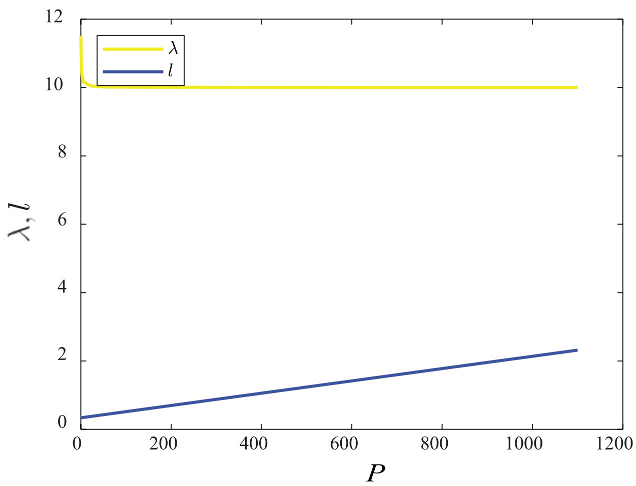

Figure 7. Graph of λ, l with respect to P.

Table 4. Hypothetical numerical values of set S_3 and set S_4

P_i :	$P_1 = 200$	$P_2 = 400$	$P_3 = 600$	$P_4 = 800$	$P_5 = 1000$
λ_i :	$\lambda_1 = 2.041$	$\lambda_2 = 2.021$	$\lambda_3 = 2.011$	$\lambda_4 = 2.010$	$\lambda_5 = 2.008$
l_i :	$l_1 = 0.6977$	$l_2 = 1.0577$	$l_3 = 1.4177$	$l_4 = 1.7777$	$l_5 = 2.1377$

Illustration 2

Let the values of variables that appeared in equations (4.1)–(4.5) be: $(a, b, c) = (1, 1, 1)$, $K = 15\ N/m$, $g = 9.8\ m^2/s$, $X = 30$, $\alpha = 1$, $\beta = 2$, $C = 5 \times 10^{-5}\ m^2$, $e = 0.35$, $D = 4 \times 10^{-4}\ mm$, $Y = 0.6\ m$.

The following table is obtained by substituting the above values of variables in the expressions of λ and l with each value of rainfall amount taken from the set P:

Fitting the curve after plotting the points in Table 4 by using Matlab software. The approximate threshold value of rainfall is $P_f = 954\ mm$ (intersection point of curves l and λ), as the curve associated with parameter l surpasses the curve associated with safety factor λ for the first time at the intersection point (see Figure 8).

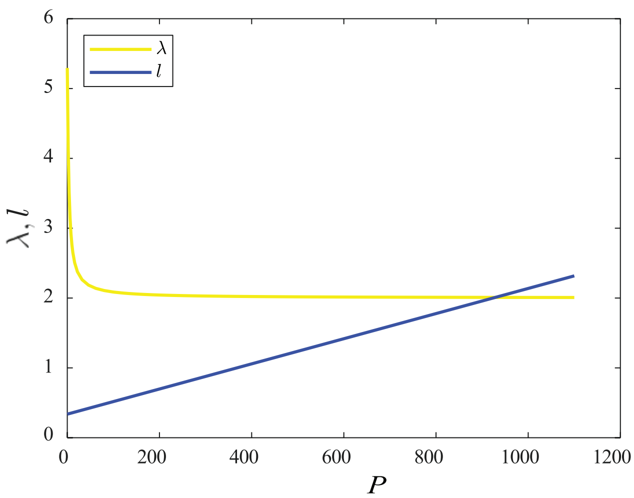

Figure 8. Graph of λ, l with respect to P.

A Comparative Study for Examining The Effectiveness Of The Present Graphical Method In Landslide Prediction With A Case Study In The Darjeeling Himalayas, India (2010–2016)

The case study suggests a specific rainfall threshold of 36.7 mm over 48 hours for landslide initiation in the Kalimpong region of the Darjeeling Himalayas during the years 2010–2016 [30].

The range of the rainfall amount is R_c = [32 mm, 143.1 mm], and the partition of the range of the rainfall amount is given as $P_c = \{30, 40, 50, 60, 70\}$, taken from the above-mentioned case study.

The expressions for safety factor λ and parameter l, respectively, can be written from equations (3.3) and (3.4) and

Figures 5 and 6 are as follows:

$$\lambda = \{(a - bP)/c + \sqrt{(bP + a)^2/c^2 + \frac{2K}{cg\sin X} h(\Omega)}\}. \quad (5.1)$$

$$h(\Omega) = \frac{4 - \pi}{(\alpha + \beta) - \sqrt{(\alpha - \beta)^2 + \pi\alpha\beta}}. \quad (5.2)$$

$$l = \frac{R + h_c - Y}{\sin X}. \quad (5.3)$$

Where,

$$R = 0.0018P - 0.0193. \quad (5.4)$$

$$h_c = \frac{C}{eD_{10}}. \quad (5.5)$$

Let the values of variables that appeared in equations (5.1)–(5.5) be: $(a, b, c) = (1, 1, 1)$, $K = 15\ N/m$, $g = 9.8\ m^2/s$, $X = 10$, $\alpha = 1$, $\beta = 2$, $C = 5 \times 10^{-5}\ m^2$, $e = 0.35$, $D_{10} = 4 \times 10^{-4}\ mm$, $Y = 0.06\ m$.

The following table is obtained by substituting the above values of variables in the expressions of λ and l with each value of rainfall amount taken from the set P_c:

Fitting the curve after plotting the points in Table 5 by using Matlab software. The approximate threshold value of rainfall is $P_f = 32.22\ mm$ (intersection point of curves l and λ), as the curve associated with parameter l surpasses the

Table 5. Numerical values of set S_3 and set S_4 obtained from the case study

P_i :	$P_1 = 30$	$P_2 = 40$	$P_3 = 50$	$P_4 = 60$	$P_5 = 70$
λ_i :	$\lambda_1 = 2.041$	$\lambda_2 = 2.021$	$\lambda_3 = 2.011$	$\lambda_4 = 2.010$	$\lambda_5 = 2.008$
l_i :	$l_1 = 2.009$	$l_2 = 2.112$	$l_3 = 2.215$	$l_4 = 2.318$	$l_5 = 2.421$

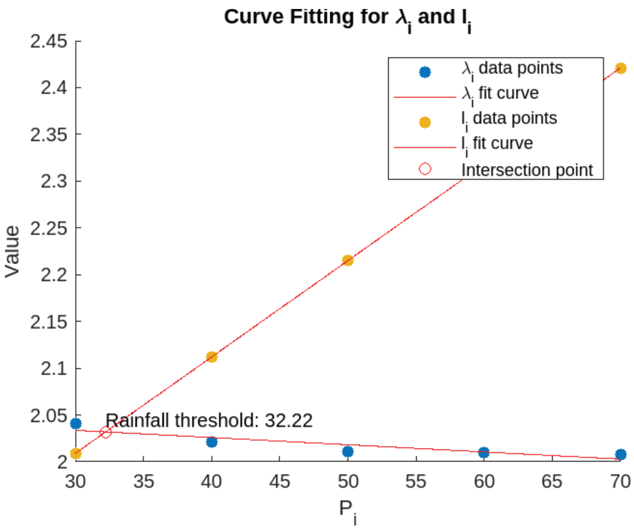

Figure 9. Graph of λ, l with respect to P.

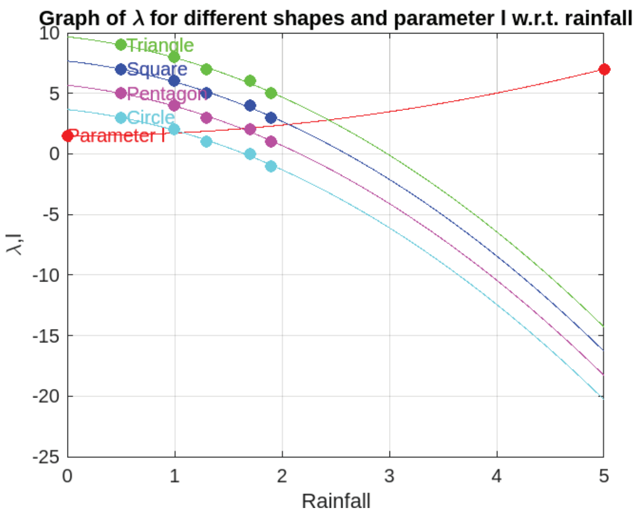

Figure 10. Graph of λ for different shapes and parameter l with respect to rainfall.

curve associated with safety factor λ for the first time at the intersection point (see Figure 9).

The calculated threshold using this graphical method closely aligns with the value suggested by earlier studies, standing at 32.22 mm, a figure notably close to the previously established threshold of 36.7 mm. This congruence not only underscores the robustness and validity of the proposed graphical method but also highlights its effectiveness in accurately predicting landslide triggers in the region. The consistency between the findings of this method and the results of prior research reinforces confidence in our understanding of landslide dynamics in the Kalimpong Region.

The proposed graphical method for determining the rainfall threshold for landslide initiation requires data on rainfall amount (P), the generalized Cheeger constant (λ) of domain D, and the parameter l, which represents the geological material content within domain D. In this comparative study, rainfall data from the Kalimpong Region of the Darjeeling Himalayas from 2010 to 2016 is used. This study assumes that the relationship between rainfall and groundwater table is similar to that of the site named Jiuqu in the Dashu district of Kaohsiung City,

Southern Taiwan, for the evaluation of parameter l, enabling comparison. The comparative study is tailored for the locations of the Kalimpong Region of the Darjeeling Himalayas, where the geographical characteristics align closely with the values of variables used in the determination of the generalized Cheeger constant. This similarity enhances the relevance and significance of the comparative study, providing valuable insights into landslide susceptibility and rainfall thresholds for regions with comparable geological and topographical features.

RESULTS AND DISCUSSION

Implications of Geometric Shapes on the Rainfall Threshold

As the number of sides of the regular polygon of the same area increases, the value of the Cheeger constant decreases, and the disk exhibits the least value among all shapes of the same area. Suggesting that the value of the rainfall threshold of the domain with a circular-shaped base is the least among all bases of the same area and that of the domain with an equilateral triangular-shaped base is the largest among all bases (having the shape of a regular polygon) of the same area, the value of the rainfall threshold decreases for the domain whose base (of equal area) is in the form of a regular polygon as the number of sides of the regular polygon increases. Thus, the current study gives important and interesting insights into the interplay between geometric shapes, their Cheeger constants, and the associated implications for rainfall thresholds in landslide prediction (see Figure 10).

Extension to Dynamic Generalized Cheeger Problems

The current study makes a notable extension of the classical study of generalized Cheeger problems to dynamic investigations. The present study ventures into the dynamic zone instead of usual static approaches, making simple classical Cheeger problems into a more versatile concept that allows the applicability of the generalized Cheeger concept for addressing complex and dynamic problems.

Exploration of Real-Life Applications

An honest attempt has been made in this paper to draw out more real-life applications emanating from simple classical Cheeger problems. The present study bridges the gap between pure mathematical concepts and practical benefits.

The endeavor is to understand the utility of Cheeger problems in diverse real-world applications.

Novelty in the Dynamic Generalized Cheeger Problem

A unique dynamic approach for the study of the generalized Cheeger problem departing from traditional approaches of static nature for the classical Cheeger problem leads to the development of an innovative graphical method for temporal landslide prediction and rainfall threshold determination, which preserves the novelty of the present study, thereby enhancing the potentiality of the simple classical Cheeger problem to predict physical phenomena.

Significance of the Dynamic Generalized Cheeger Problem

The driving force to dig into the dynamic generalized Cheeger problem originates from a recognition of its intrinsic worth. The developed approach has the potential to reveal fresh perspectives, not only enhancing the capabilities of predicting spatial and temporal landslides but also opening routes for entirely new areas of research. The dynamic nature of the current study offers a promising pathway to the development of innovative methods and techniques.

Computational Efficiency of the Graphical Method

The peculiar traits of the proposed graphical method are that it is simple to understand, easy to operate, and involves less computational cost, making it an approachable and handy option for researchers seeking efficient methods for predicting temporal landslides and rainfall thresholds.

Effectiveness of the Graphical Method in Determining Threshold Rainfall

The comparative study underscores the effectiveness of the graphical method in determining threshold rainfall for landslide initiation. The threshold value determined through this graphical approach is strikingly similar to the one proposed in earlier research, standing at 32.22 mm. This figure closely mirrors the previously established threshold of 36.7 mm. The close alignment of the calculated threshold rainfall values with those derived from previous studies reaffirms the reliability and accuracy of this method.

CONCLUSION

This paper has proposed the novel idea of studying the dynamic generalized Cheeger problem and developed a graphical method to predict temporal landslides and rainfall thresholds, respectively. The results of the current study provide valuable insights into the findings of the present research. The numerical illustrations provided demonstrate the reliability and robustness of the current study.

The numerical illustrations presented analyze discrete data of rainfall amount alongside corresponding values of safety factor λ and parameter l, representing geological material content within domain D. Curve fitting applied to these datasets reveals critical insights into landslide susceptibility. In Illustration 1, where the curve associated with parameter l consistently remains below that of safety factor λ, the hypothetical natural structure is deemed safe throughout the observed rainfall period. Conversely, in Illustration 2, the intersection point of the curves signifies an approximate rainfall threshold ($P_f = 954\ mm$), marking the point at which the curve associated with parameter l surpasses that of safety factor λ for the first time. These findings offer valuable guidance for landslide risk assessment, aiding in the identification of critical rainfall thresholds and forming effective mitigation strategies. Moreover, the comparative study demonstrates the effectiveness of the graphical method in determining threshold rainfall for landslide initiation in the Kalimpong Region of the Darjeeling Himalayas by utilizing data from 2010 to 2016. The threshold value derived using this graphical method closely resembles the figure suggested by prior research, measuring 32.22 mm. This result is remarkably close to the established threshold of 36.7 mm, reinforcing the reliability and consistency of the findings.

Future Directions and Potential Extensions:

The idea of studying the time-varying (dynamic) generalized Cheeger problem is worthy of doing, as it may reveal new insights into developing new tools not only for temporal and spatial prediction of landslides but also for an entirely new area of research. The dynamic study of the generalized Cheeger problem may emerge as a useful and versatile tool for unknotting intricate challenges across diverse research domains in the near future. While the current study adheres to the usual metric space, by changing the metric space, it can unlock solutions to numerous problems in diverse fields. A dynamic study of the generalized Cheeger problem has great scope for future work. Temporal and spatial landslide prediction can be done with different landslide triggering factors, either one at a time or with multiple factors simultaneously, for better predictions with real data. The threshold value of a single landslide triggering factor can be calculated with the proposed graphical method, and this deterministic model can be integrated with some other probabilistic models to get better temporal and spatial landslide prediction and forecasting.

AUTHORSHIP CONTRIBUTIONS

Authors equally contributed to this work.

DATA AVAILABILITY STATEMENT

The authors confirm that the data that supports the findings of this study are available within the article.

CONFLICT OF INTEREST

The author declared no potential conflicts of interest with respect to the research, authorship, and/or publication of this article.

ETHICS

There are no ethical issues with the publication of this manuscript.

FUNDING

This research received no external funding.

REFERENCES

[1] Aristizábal E, Sánchez O. Spatial and temporal patterns and the socioeconomic impacts of landslides in the tropical and mountainous Colombian Andes. Disasters 2020;44:596–618. [CrossRef]
[2] Badoux A, Andres N, Techel F, Hegg C. Natural hazard fatalities in Switzerland from 1946 to 2015. Nat Hazards Earth Syst Sci 2016;16:2747–2768. [CrossRef]
[3] Donnini M, Modica M, Salvati P, Marchesini I, Rossi M, Guzzetti F, Zoboli R. Economic landslide susceptibility under a socio-economic perspective: an application to Umbria Region (Central Italy). Rev Reg Res 2020;40:159–188. [CrossRef]
[4] Yang HQ, Zhang L, Gao L, Phoon KK, Wei X. On the importance of landslide management: Insights from a 32-year database of landslide consequences and rainfall in Hong Kong. Eng Geol 2022;299:106578. [CrossRef]
[5] Jiao Q, Jiang W, Qian H, Li Q. Research on characteristics and failure mechanism of Guizhou Shuicheng landslide based on InSAR and UAV data. Nat Hazards Res 2022;2:17–24. [CrossRef]
[6] Song Y, Fan W, Yu N, Cao Y, Jiang C, Chai X, Nan Y. Rainfall induced shallow landslide temporal probability modelling and early warning research in mountains areas: A case study of Qin-Ba Mountains, Western China. Remote Sens 2022;14:5952. [CrossRef]
[7] Yamagishi H, Marui H, Ayalew L, Sekiguchi T, Horimatsu T, Hatamoto M. Estimation of the sequence and size of the Tozawagawa landslide, Niigata, Japan, using aerial photographs. Landslides 2004;1:299–303. [CrossRef]
[8] Galeria del Ministerio de Defensa del Peru. Available at: https://www.flickr.com/photos/ministeriodedefensaperu/39935939755/in/date Accessed May 14, 2025.
[9] Cazacu O, Cristescu N. Constitutive model and analysis of creep flow of natural slopes. Ital Geotech J 2000;34:44–54.
[10] Cristescu ND, Cazacu O, Cristescu C. A model for slow motion of natural slopes. Can Geotech J 2002;39:924–937. [CrossRef]
[11] Hild P, Ionescu IR, Lachand-Robert T, Roşca I. The blocking of an inhomogeneous Bingham fluid. Applications to landslides. ESAIM Math Model Numer Anal 2002;36:1013–1026. [CrossRef]
[12] Ionescu IR, Lachand-Robert T. Generalized Cheeger sets related to landslides. Calc Var Partial Differ Equ 2005;23:227–249. [CrossRef]
[13] Ionescu IR, Lupaşcu O. Onset of a dense avalanche on a plane slope. Proc Romanian Acad Ser A 2015;16:405–412.
[14] Cheeger J. A lower bound for the smallest eigenvalue of the Laplacian. In: Problems in Analysis: A Symposium in Honor of Salomon Bochner. Princeton Univ Press 2015:195–200. [CrossRef]
[15] Demengel F. On some nonlinear equation involving the 1-Laplacian and trace map inequalities. Nonlinear Anal Theory Methods Appl 2002;48:1151–1163. [CrossRef]
[16] Kawohl B, Fridman V. Isoperimetric estimates for the first eigenvalue of the p-Laplace operator and the Cheeger constant. Comment Math Univ Carol 2003;44:659–667.
[17] Kawohl B, Lachand-Robert T. Characterization of Cheeger sets for convex subsets of the plane. Pac J Math 2006;225:103–118. [CrossRef]
[18] Krejčiřík D, Pratelli A. The Cheeger constant of curved strips. Pac J Math 2012;254:309–333. [CrossRef]
[19] Leonardi GP, Neumayer R, Saracco G. The Cheeger constant of a Jordan domain without necks. Calc Var Partial Differ Equ 2017;56:164. [CrossRef]
[20] Parini E. An introduction to the Cheeger problem. Surv Math Appl 2011;6:9–21.
[21] Ionescu IR, Lupaşcu-Stamate O. Boundary variation method for the generalized Cheeger problem. Appl Numer Math 2019;140:199–214. [CrossRef]
[22] Mandal S, Mondal S. Statistical Approaches for Landslide Susceptibility Assessment and Prediction. New York: Springer Int Publication; 2019. [CrossRef]
[23] Bingham EC. Fluidity and Plasticity. New York, London: McCraw-Hill Book Company; 1922.
[24] Oldroyd JG. A rational formulation of the equations of plastic flow for a Bingham solid. Math Proc Camb Philos Soc 1947;43:100–105. [CrossRef]
[25] Drucker DC, Prager W. Soil mechanics and plastic analysis of limit design. Q Appl Math 1952;10:157–165. [CrossRef]
[26] Chowdhury R, Bhattacharya G, Flentje P. Geotechnical Slope Analysis. Boca Ratın, Florida: CRC Press; 2009. [CrossRef]
[27] Hussain F, Wu RS, Shih DS. Water table response to rainfall and groundwater simulation using physics-based numerical model: WASH123D. J Hydrol Reg Stud 2022;39:100988. [CrossRef]
[28] Li Y, Zhang C, Chen C, Chen H. Calculation of capillary rise height of soils by SWCC model. Adv Civ Eng 2018;2018:190354. [CrossRef]
[29] Todisco F, Lorenzo V, Alessandra V, Dino T. Infiltration and bulk density dynamics with simulated rainfall sequences. Catena 2022;218:106542. [CrossRef]
[30] Teja TS, Surya T, Dikshit A, Satyam N. Determination of rainfall thresholds for landslide prediction using an algorithm-based approach: Case study in the Darjeeling Himalayas, India. Geosci 2019;9:302. [CrossRef]
[31] Highland LM, Bobrowsky P. O Manual de Deslizamento – Um Guia para a Compreensão de Deslizamentos. US Geol Surv Circ 2008;1325.

APPENDIX A

In Appendix A, a brief account of the various causes and triggering factors of landslides is given as A.1 [31] and the relationship between causal factors of landslides and landslide predicting parameters involved in the present study as A.2 in the tabulation form, respectively.

A.1 Various Causes and Triggering Factors of Landslides

1 GROUND CONDITIONS

1.1 Collapsible material, plastic fragile substance, sensitive substance, sheared ma- terial, weathered substance, and fissured/jointed substance.

1.2 Structural discontinuities (including faults, unconformities, flexural shears, sed- imentary contacts) and adversely oriented mass discontinuities (including bed- ding, schistosity, cleavage).

1.3 Effects of permeability contrast and stiffness contrast on ground water (stiff, dense substance over plastic substance).

2 GEOMORPHOLOGICAL CAUSES

2.1 Tectonic uplift and volcanism.

2.2 Crustal rebound.

2.3 Erosion of the slope toe due to wave, glacier, and streamflow.

2.4 Subterranean erosion and lateral margin erosion (solution, pipes).

2.5 The slope's or its crest's deposition loading.

2.6 Removal of vegetation due to erosion, forest fires, and dryness.

3 PHYSICAL CAUSES FOR LANDSLIDE

3.1 High precipitation and intense rainfall.

3.2 Rapid melting of deep snow.

3.3 Rapid drawdown after floods, high seas and natural dam breaches, etc.

3.4 Volcanic eruption and earthquake.

3.5 The weathering of expansive soils and the breaching of crater lakes.

3.6 Permafrost thawing and freeze-thaw weathering.

3.7 Shrink-and-swell weathering and freeze-and-thaw weathering.

4 MAN-MADE CAUSES FOR LANDSLIDING

4.1 Removal of vegetation/deforestation.

4.2 Quarrying, mining and generation of dumps for the settlement of loose waste.

4.3 Man-made vibrations (heavy machinery, traffic, pile driving).

4.4 Road and building constructon at hilly places.

4.5 Poor maintenance of drainage system and leakage of water from various services.

4.6 Drawdown of reservoirs and irrigation.

4.7 Loading of the slope or Unearthing of the slope.

4.8 Bad agricultural practices.

A.2 Relationship Between Landslide Predicting Parameters in the Present Study and Causal Factors of Landslides